Ibn Al-Haitham Journal for Pure and Applied Sciences
Journal homepage: jih.uobaghdad.edu.iq
PISSN: 1609-4042, EISSN: 2521-3407
IHJPAS. 2025, 38(3)

The Effect of Ferric Oxide Nanoparticles on *Candida albicans*

Rima Mohamed Yehia Nasif[1*] and Hassan Majeed Rasheed [2]
[1,2]Department of Biology, College of Science, University of Baghdad, Baghdad, Iraq.
*Corresponding Author.

Received: 11 September 2023 Accepted: 28 November 2023 Published: 20 July 2025
doi.org/ 10.30526/38.3.3684

Abstract

The biosynthesis of nanoparticle-mediated pigments has been widely used as an antimicrobial agent against microorganisms.In order to study the effect of ferric oxide (Fe_2O_3) nanoparticles on *Candida albicans*, they were biosynthesized by using pyocyanin pigment produced from *Pseudomonas aeruginosa*. Fe_2O_3NPs were characterized by using atomic force microscopy (AFM), Fourier transform-infrared spectroscopy (FTIR), Field Emission Scanning Electron Microscope (FE-SEM), Energy Dispersive X-ray Spectroscopy (EDX), and UV-Visible spectroscopy. From December 2022 to July 2023, a total of 48 samples of C. albicans were collected from burns, wounds, and urine from private labs and Al-Kindy hospital; only 19 were identified as C. albicans isolates according to the cultural and morphological characteristics and VITEK-2 system. For the antimicrobial effect, they were cultured on Mueller Hinton agar using the agar well diffusion method.The results provided evidence that the diameter of the inhibition zone was directly proportional to the concentration; at 0.1 µg/ml, the diameter of the inhibition zone was 30 mm, while at 0.0125 µg/ml, the diameter was 14 mm.The study confirms the concentration-dependent antifungal effect of Fe_2O_3 nanoparticles synthesized by biological methods, suggesting potential applications in antifungal therapy.

Keywords: Ferric oxide, nanoparticles, *Candida albicans*, pyocyanin, biosynthesis, *Pseudomonas aeruginosa*

1. Introduction

Nanotechnology encompasses the scientific, technical, and technological activities that occur at the nanoscale. A wide range of scientific fields, from chemistry and biology to physics and materials science to engineering, can benefit from it. Nanoparticles (NPs) are substances characterized by having two or more dimensions, often with a diameter falling within the range of 1-100 nm (1). *Ex vivo* (out of the living) synthesis of NPs is becoming increasingly popular for various uses, including medical treatments, industrial production and incorporation into materials such as cosmetics or clothing. Increased reactivity and possible biochemical activities

result from the high surface-to-volume ratio of NPs. However, the underlying chemical mechanisms of how NPs interact with biological systems are mainly undiscovered (2).

Antifungals are used as a treatment for invasive candidiasis. Nevertheless, prolonged or exaggerated use of these medications caused the development of resistant organisms and treatment failure, which is why it is crucial to identify alternative antifungal medicines with fewer adverse effects (3).

Part of hospital-acquired infections are caused by the genus *Candida*, which is a yeast that can cause opportunistic infections in immunocompromised hosts like those with HIV/AIDS, cancer, major surgery, and transplant recipients on immunosuppressive therapy; over 90% of invasive candidiasis infections are caused by *Candida albicans* and non-albicans C. spp., including *C. lusitaniae, C. krusei, C. tropicalis, C. glabrata, and C. parapsilosis*(3). *C.albicans* are considered a normal flora in humans and reside in the alimentary canal, respiratory tract, and female genital system, as well as on the skin (4).

2. Materials and Methods

2.1 Isolation and Identification of *Candida albicans*

Samples from wounds, burns, and urinary tract infections were obtained from patients in private labs and Al-Kindy hospital, then were cultured on chromogenic agar for detection and identification of *C.albicans*. The duration of the trial was from December 2022 to July 2023.

2.2 Morphology Characteristics

Yeast cells were stained with Gram stain or lactophenol cotton blue and examined under the microscope to determine the identity of *Candida* species and other yeast colonies grown on UTI chromogenic agar **(Figure 1).**

Figure 1. *Candida* on Chrom agar

2.3 Identification by VITEK -2 system

Candida albicans was identified, sensitivity was tested, and colonies were counted using the Vitek-2 technique. Solutions were prepared, samples were incubated before application, cards were sealed and incubated, the optical system was adjusted, test reactions were applied, and analytical techniques were used per the company's regular manufacturing guidelines (5).

2.4 Preparation of Ferric Oxide Nanoparticles (Fe_2O_3 NPs)

The first step in nanoparticle preparation is preparing a flask that contains 150 ml of chloroform containing pyocyanin and 15 g of ferric chloride. The flasks were placed intermittently in a sonicator (every 30 sec.) for 15 minutes, then placed in a shaker for 48 hours. After 48 hours of shaking, both of the solutions in each flask were poured into plain tubes, about 5 ml in each tube, The tubes were placed in a centrifuge for 5000 rpm for minute, washed with DDW, and placed again in the centrifuge for 5000 rpm/10 minute then washed and centrifuged again. The solution was placed in a petri dish and left to dry in an incubator(6).

2.5 Characterization techniques

1. Atomic force microscopy (AFM) analysis (Angstrom advanced, USA)
2. FTIR (Fourier Transform Infrared Spectroscopy) (SHIMADZU, Japan)
3. Field Emission Scanning Electron Microscope (FESEM) (Tescan Netherlands)
4. Energy-dispersive X-ray spectroscopy (Panalytical, Almelo, Netherlands),
5. UV–VIS spectral analysis pyocyanin (SHIMADZU, Japan)

2.6 Antimicrobial activity of prepared nanoparticles

The antimicrobial efficacy of Fe_2O_3NPs was examined using agar well diffusion method to determine the minimum inhibition concentration of Fe_2O_3 nanoparticles for the test microorganism(7), a stock solution was prepared of 1 gram of Fe_2O_3NPs then dilute the stock solution 1:10 to obtain a concentration of 0.1 CFU/mL, dilute the 0.1 CFU/mL solution 1:2 to obtain a concentration of 0.05 CFU/mL, dilute the 0.05 CFU/mL solution 1:2 to obtain a concentration of 0.025 CFU/mL, dilute the 0.025 CFU/mL solution 1:1.4 to obtain a concentration of 0.014 CFU/mL and finally dilute the 0.014 CFU/mL solution 1:1.25 to obtain a concentration of 0.0125. Muller- Hinton agar medium (25mL) was sterilized, cooled, and then the liquid was carefully transferred into sterilized Petri plates and afterwards left undisturbed to harden at the room temperature. Sterile cotton swabs were used to transfer and spread the overnight growth of test microorganisms onto the agar medium according to McFarland ($1.5*10^8$ CFU/ml). Wells were made in agar by using cork borer and filled with various concentrations test (0.1,0.05, 0.025, 0.014, and 0.0125 µg /ml) of Fe_2O_3 nanoparticles CFU/mL.as well as using control of ferric oxide, Placed in incubator for 24hr at 37 C°.

3. Results

3.1 Morphological tests result

Morphologically, the hyphae were constricted at regular intervals, giving them the appearance of sausage links, and budding yeast forms (blastoconidia) were commonly seen. The yeast was germ tube positive as evidenced by the development of a cylindrical filament from the blastoconidium without constriction at the location of origin and without apparent swelling along the length of the filaments (8).

3.2 Identification by Vitek-2 system

Isolates were confirmed as being *Candida albicans* by using Vitek-2 system as the **Figure (2)**.

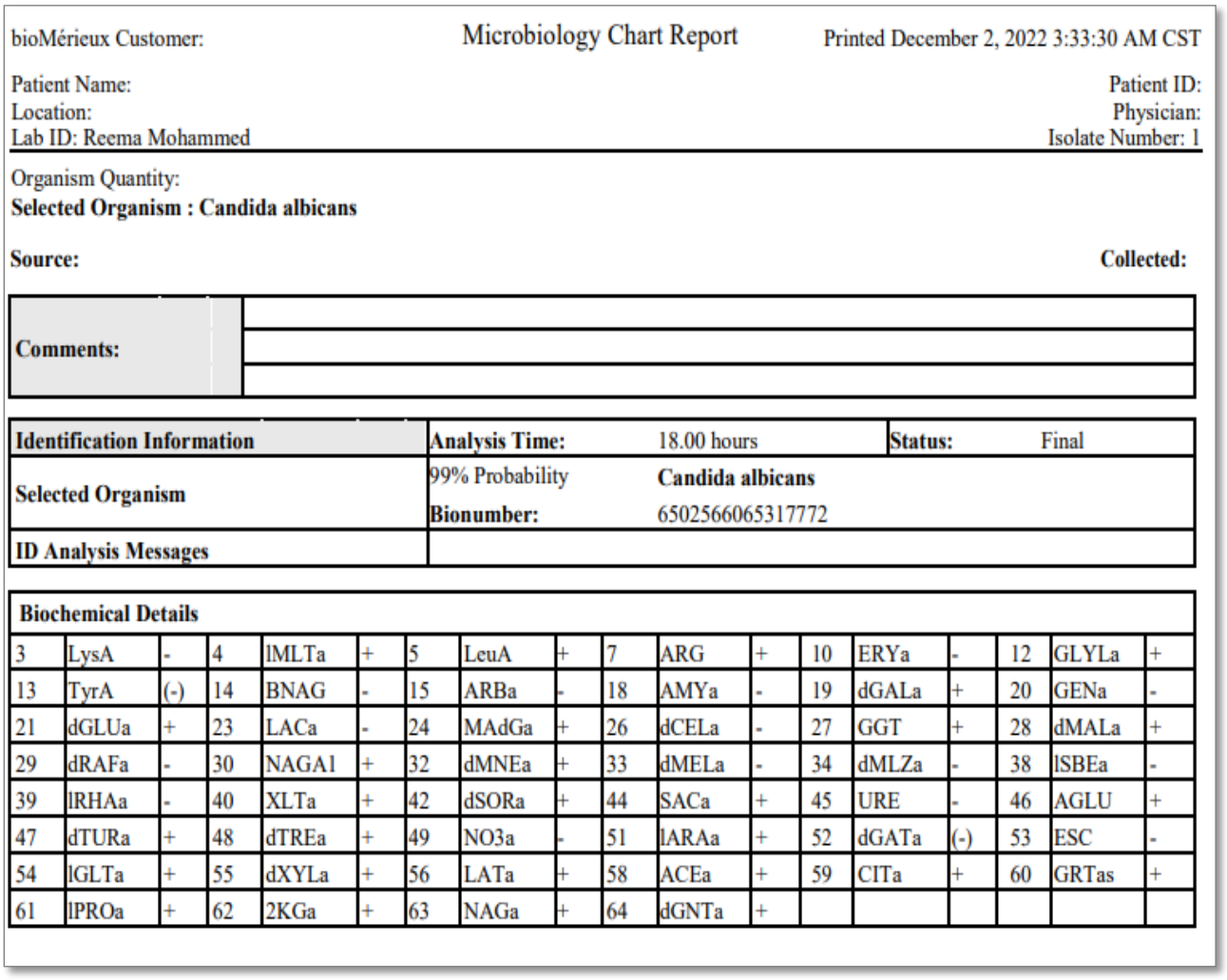

bioMérieux Customer: Microbiology Chart Report Printed December 2, 2022 3:33:30 AM CST

Patient Name: Patient ID:
Location: Physician:
Lab ID: Reema Mohammed Isolate Number: 1

Organism Quantity:
Selected Organism : Candida albicans

Source: **Collected:**

Comments:	

Identification Information	**Analysis Time:**	18.00 hours	**Status:**	Final
Selected Organism	99% Probability	**Candida albicans**		
	Bionumber:	6502566065317772		
ID Analysis Messages				

Biochemical Details

3	LysA	-	4	lMLTa	+	5	LeuA	+	7	ARG	+	10	ERYa	-	12	GLYLa	+
13	TyrA	(-)	14	BNAG	-	15	ARBa	-	18	AMYa	-	19	dGALa	+	20	GENa	-
21	dGLUa	+	23	LACa	-	24	MAdGa	+	26	dCELa	-	27	GGT	+	28	dMALa	+
29	dRAFa	-	30	NAGA1	+	32	dMNEa	+	33	dMELa	-	34	dMLZa	-	38	lSBEa	-
39	lRHAa	-	40	XLTa	+	42	dSORa	+	44	SACa	+	45	URE	-	46	AGLU	+
47	dTURa	+	48	dTREa	+	49	NO3a	-	51	lARAa	+	52	dGATa	(-)	53	ESC	-
54	lGLTa	+	55	dXYLa	+	56	LATa	+	58	ACEa	+	59	CITa	+	60	GRTas	+
61	lPROa	+	62	2KGa	+	63	NAGa	+	64	dGNTa	+						

Figure 2. Identification of *Candida albicans* by Vitek-2 system

3.3 Characterisitcs of nanoparticles

3.3.1 Atomic force microscopy (AFM) analysis

Atomic force microscopy (AFM) was used to determine the size and surface morphology of ferric oxide NPs nanoparticles, testing the contact forces between the tip and surface (9). **Figures (3)** and **(4).** illustrates two and three dimensional AFM of ferric oxide NPs which were all the same shape and size. Also, the average size of biosynthesized Ferric oxide NPS by pyocyanin according to **Table (1)** was 39.26 nm.

Table 1. The Cumulation size of Ferric Oxide Nanoparticles Biosynthesized by pyocyanin by AFM technique.

Avg.Diameter:39.26 nm	<=10% Diameter: 18:00 nm
<=50% Diameter:36.00 nm	<=90% Diameter: 60:00 nm

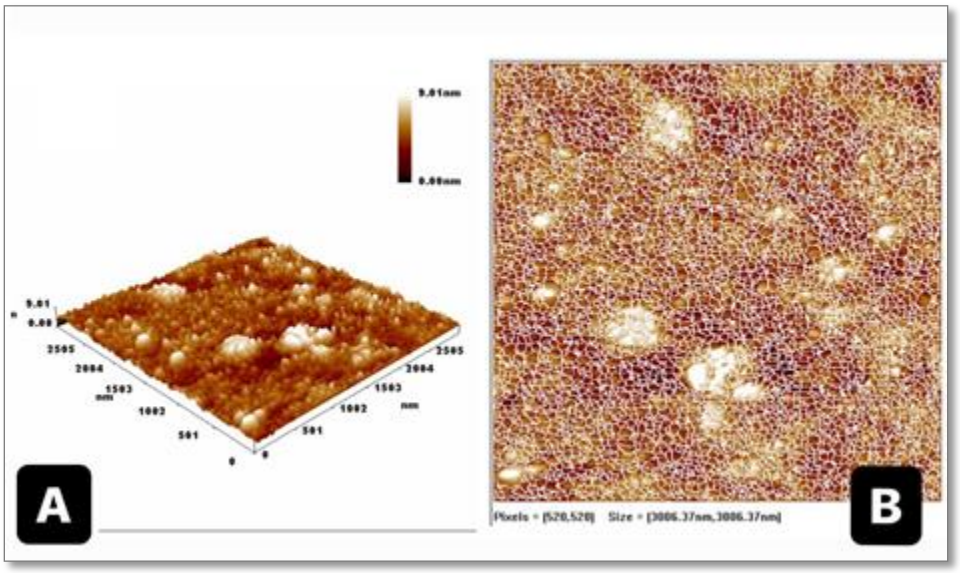

Figure 3. The biosynthesized Ferric oxide NPs (A)(B) 2D and 3D AFM of ferric oxide NPs.

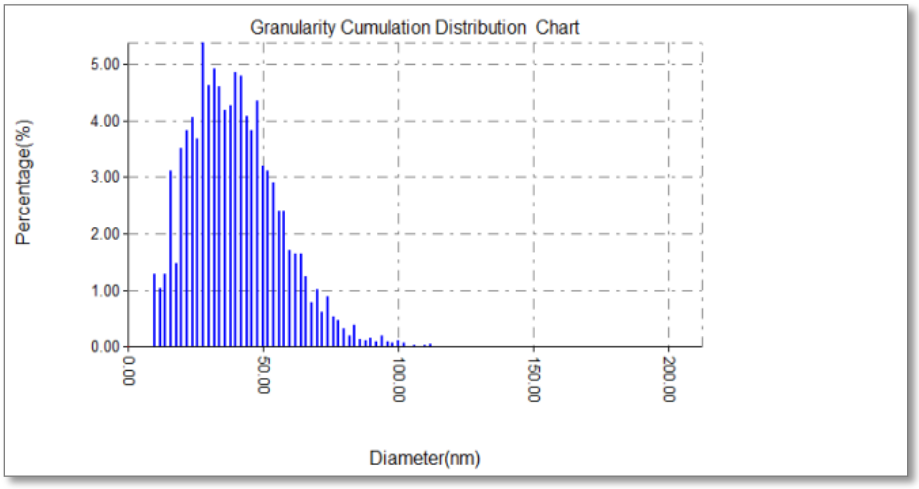

Figure 4. Chart Granularity Distribution of ferric oxide NPs

The result is in correlation with (1) AFM result which showed that the average Ferric oxide nanoparticles size was in a range from 20-40 nm.

3.3.2 Fourier Transform Infrared Spectroscopy (FTIR)

The bond vibration frequencies can be calculated using FTIR spectrographic investigation. In addition, the synthesized Fe_2O_3 nanoparticles' infrared-optimized band value was supported by the chemical functional group of Fe_2O_3 nanoparticles. The existence of Fe_2O_3 bonding was verified by FTIR as in **Table (2)**.

Table 2. FTIR of Fe_2O_3 nanoparticles

Type of compound	Frequency of Absorption (cm^{-1})	Bonds	Compound class of Functional Groups
Pyocyanin	3421.48-3406.05	O-H stretching	Alcohol
	2954.74-2854.45	O-H stretching (strong broad), O-H stretching (weak broad), N-H stretching, C-H stretching	Carboxylic acid, alcohol, amine salt, alkane
	1110.92-1033.77	C-F stretching	Fluoro compound
Pyocyanin +Ferric sulphate	3433.06	O-H stretching	alcohol
	2925.81-2854.45	O-H stretching N-H stretching C-H stretching	carboxylic group, alcohol amine salt alkane
	1629.74	O-H stretching C=C stretching	intramolecular bonded cyclic alkane, conjugated alkene
	1490.87-1433.01	N-H bending C-H bending	amine alkane
	1083.92-1029.92	C-F stretching C-N stretching	fluoro compound amine salt
Ferric sulphate	536.17-426.24		Metal oxide
	3390.63-3367.48		
	1677.95-1649.02	C-H bending C=N stretching	aromatic compound imine \oxime
	1091.63	C-O stretching C-N stretching C-F stretching	aliphatic ether, secondary alcohol amine fluoro compound
	671.18-526.53	C-Br stretching	halo compound
Fe_2O_3 NPs	3541.06-3253.69	O-H stretching	alcohol
	1650.95-1622.02	*C-H bending, C=C stretching	Aromatic compound, conjugated alkene
	1103.21	C-O stretching, C-F stretching, C-N stretching	Aliphatic ether, secondary alcohol Fluoro compound, amine
	613.32	C-Br stretching	*halo compound

3.3.3 Field Emission Scanning Electron Microscope (FESEM)

The FE-SEM image in **Figure (5)** reveals that ferric oxide NPs are both uniformly distributed and almost perfectly spherical in shape. The average particle size is about 38.01 nm, and there are some NPs that have a hexagonal form.

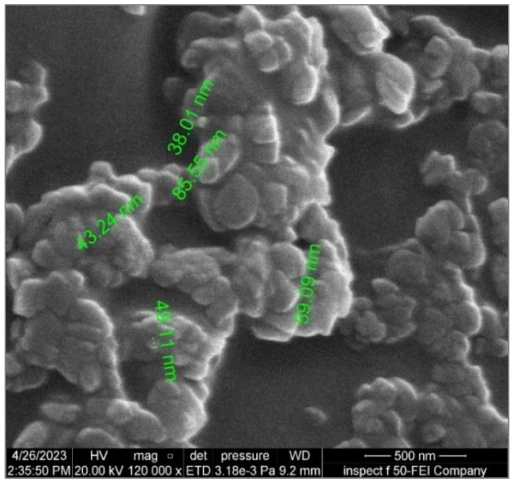

Figure 5. Field emission scanning electron microscopy images of Ferric Oxide NPs**.**

The result is in line with study which (10) revealed that the biosynthesized ferric oxide NPs had spherical shape and showed less aggregation of particles with diameters about 20-60 nm.

3.3.4 Energy-dispersive X-ray spectroscopy

The EDX plot of the SEM images used to determine the elemental composition of the Fe_2O_3NPs is depicted in **Figure (6).** High purity for the synthesized ferric oxide NPs was verified by the EDX spectra, which show that the necessary phases of Fe and O are present in the samples, as shown in **Table (3).**

Table 3. Elemental composition of the Fe_2O_3 NPs**.**

Element	Atomic %	Atomic % Error	Weight %	Weight % Error
C	21.7	0.4	15.7	0.3
O	72.4	0.5	69.7	0.5
S	3.8	0.0	7.3	0.1
Fe	2.2	0.0	7.3	0.1

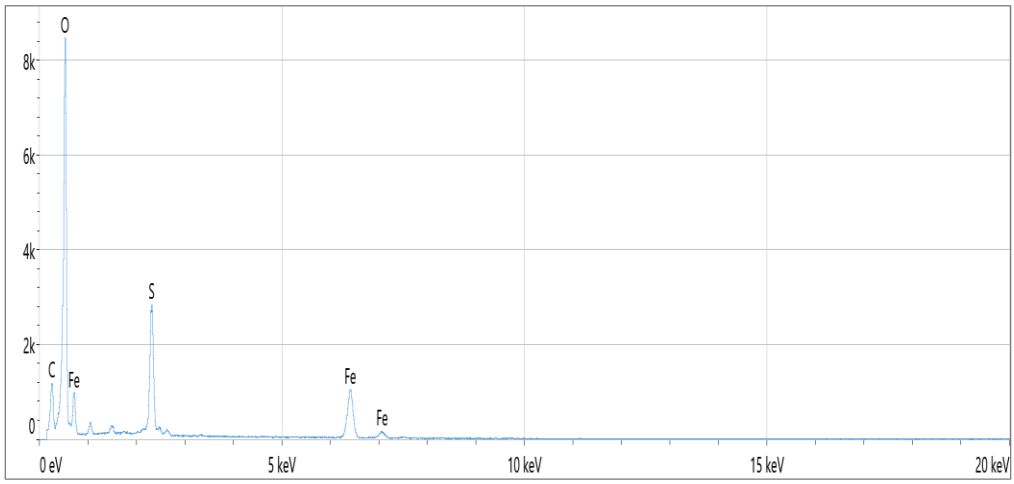

Figure 6. Diagram of elements analysis of Fe_2O_3 nanoparticles by using Energy-dispersive X-ray spectroscopy.

3.3.5 UV–VIS spectral analysis Ferric oxide

The biosynthesis Fe_2O_3 is characterized by scanning with UV-visible spectrophotometer (Shimadzu, Japan) to detect the maximum absorption. The result showed that biosynthesized Fe_2O_3NPs exhibited a maximum absorption peak at 250 nm as shown in **Figure (7).**

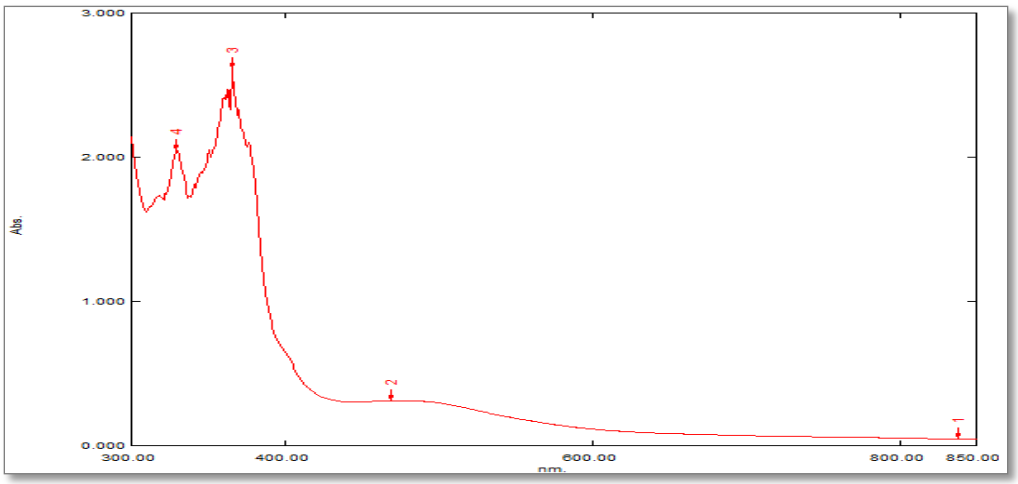

Figure 7. using the UV–Vis spectrophotometter for detecting the maximum absorption of Ferric oxide nanoparticles.

The absorption spectra at 370 nm indicate the formation of ferric oxide nanoparticle (11).The outcome was similar to a study by (12),which demonstrated that the Iron oxide NPs show absorbance 330-450 nm. Additionally, consistent with (13) investigation, which recorded that UV absorption band is observed in the region 330–450 nm

3.3.6 Determination of highest resistance isolates

The selection of the multi-drug resistant isolate was based on the outcomes obtained from the VITEK-2 system. The findings indicated that a significant proportion of isolates (85%) exhibited multidrug resistance, demonstrating resistance to a minimum of three distinct categories of the antibiotics that were tested..

3.4 Efficiency of nanoparticles against *Candida albicans*

Ferric oxide nanoparticles have exhibited antibacterial properties against *Candida albicans.*The impact of various concentrations (0.1, 0.05, 0.025, 0.014, 0.0125 µg/ml) of Fe_2O_3NPs on fungal cell viability was examined using Muller Hinton agar. The findings revealed that there is an inverse relationship between the concentration and the inhibition zone as shown in **Figure (8)** and **Table (4).** The higher the concentration, the greater the inhibtion. The strongest inhibition zone was about 30mm at 0.1 µg/ml while the weakest inhibition zone was 14 mm at 0.014 µg/ml **(Figure 9).**

The results were in excellent agreement with previous studies demonstrating the minimum inhibitory concentration of Fe_2O_3NPs (14).

The utilization of green-synthesized ferric oxide nanoparticles exhibits promising promise as an antibacterial agent for the treatment of bacterial-induced illnesses. The utilization of green synthesis presents some notable benefits in comparison to alternative methodologies. The approach employed in this study is environmentally sustainable and offers compatibility with biological systems in several fields, such as pharmaceuticals, biomedicine, and cosmetics, as it

avoids the use of hazardous chemicals during the synthesis process. The cost-effectiveness of green synthesis has also been demonstrated.

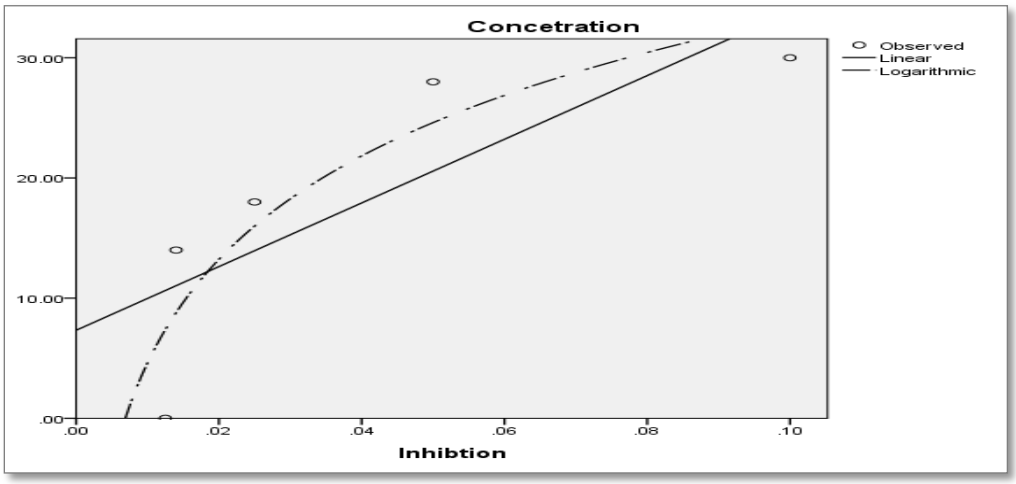

Figure 8. The relationship between concentrations and inhibition of Fe_2O_3NP

Table 4. The statistical analysis for this study

Dependent variable	**correlation**						
Equation	R Square	F	dfI	df2	Sig.	constant	B1
linear	0.644	5.419	1	3	0.102	7.325	264.897
logarithmic	0.816	13.292	1	3	0.036	61.812	12.420

Figure 9. The inhibition zones of ferric oxide nanoparticles on *Candida albicans* growing on nutrient agar.

4. Discussion

This study demonstrated that biosynthesized ferric oxide (Fe_2O_3) nanoparticles exhibit potent antifungal activity against *Candida albicans*, with a clear concentration-dependent relationship between nanoparticle dosage and inhibition zone size. The highest inhibitory effect was observed at 0.1 µg/mL, while lower concentrations showed progressively reduced zones of inhibition. These findings support the potential of Fe_2O_3 NPs as a viable alternative to traditional antifungal agents, particularly against resistant *C. albicans* strains.

The antimicrobial effect of ferric oxide nanoparticles may be attributed to their small size and large surface area, which facilitate easier penetration of microbial cell walls (15, 16). Once inside the cells, they may cause oxidative stress, disrupt membrane integrity, or interfere with essential intracellular pathways (17, 18). These mechanisms have been reported in other studies investigating metal oxide nanoparticles, which similarly confirmed size- and shape-dependent antimicrobial properties (10, 14, 19).

A significant strength of this study is the green synthesis approach using pyocyanin pigment, which avoids toxic chemicals and enhances biocompatibility. This synthesis method is environmentally friendly and cost-effective, making it suitable for large-scale application in biomedical fields (20, 21).

However, the study has certain limitations, such as the absence of *in vivo* validation, the lack of long-term toxicity data, and reliance on a single fungal species. Moreover, while the VITEK-2 system provided a robust profile of resistance patterns, broader antifungal panels and clinical correlation would strengthen the findings.

Comparative analysis with previous research revealed consistent results in terms of nanoparticle size, morphology, and UV-Vis absorbance, supporting the reproducibility of the synthesis method. The antifungal effectiveness aligns with studies on other metal-based nanoparticles like ZnO and CuO, though Fe_2O_3 offers a safer toxicity profile (22, 23, 24, 25).

In conclusion, biosynthesized Fe_2O_3 nanoparticles represent a promising antifungal candidate, especially for drug-resistant fungal infections. Future research should explore in vivo efficacy, optimize delivery methods, and assess long-term safety to facilitate clinical translation.

5. Conclusion

The use of ferric oxide nanoparticles has demonstrated significant antifungal properties against *C.albicans*, suggesting their potential as a novel therapeutic approach. The pyocyanin serves as a valubale and effecctive tool in producing nanoparticles with potential application in various field.

Acknowledgment

The authors would like to thank the staff of Al-Kindy Hospital and the supporting private laboratories for their assistance in providing clinical samples and laboratory support during the course of this research.

Conflict of Interest

The authors declare that they have no conflicts of interest.

Funding

This research received no specific grant from any funding agency in the public, commercial, or not-for-profit sectors.

Ethical Clearance

This research was subjected to ethical considerations and was approved by the Committee of Ethical Standards in the College of Science, University of Baghdad , in accordance with the form

supplied by the Iraqi Ministry of Health for this purpose.Ref :CSEC/0922/0085, 23/ September /2022.

References

1. Hassan DF, Mahmood MB. Biosynthesis of Iron Oxide Nanoparticles Using Escherichia coli. Iraqi J Sci. 2019;453–459.
2. Siddiqui MH, Al-Whaibi MH, Sakran AM, Ali HM, Basalah MO, Faisal M. Calcium-Induced Amelioration of Boron Toxicity in Radish. J Plant Growth Regul. 2013;32:61–71. doi:10.1007/s00344-012-9276-6.
3. Seddighi NS, Salari S, Izadi AR. Evaluation of Antifungal Effect of Iron-oxide Nanoparticles against Different *Candida* Species. IET Nanobiotechnol. 2017;11:883–888. https://doi.org/10.1049/iet-nbt.2017.0025
4. Katafa AJ, Hamid MK. Influence of ZnO Nanoparticles on *Candida albicans* of Human Male Pleural Fluid. Iraqi J Sci. 2020;540–549. https://doi.org/10.24996/ijs.2020.61.3.10
5. Pincus DH. Microbial Identification Using the BioMérieux Vitek® 2 System. In: Parenteral Drug Association, editor. Encyclopedia of Rapid Microbiological Methods. Bethesda, MD: Parenteral Drug Association; 2006.
6. Ezhilarasi AA, Vijaya JJ, Kaviyarasu K, Kennedy LJ, Ramalingam RJ, Al-Lohedan HA. Green Synthesis of NiO Nanoparticles Using Aegle Marmelos Leaf Extract for the Evaluation of In-Vitro Cytotoxicity, Antibacterial and Photocatalytic Properties. J Photochem Photobiol B Biol. 2018;180:39–50.
7. Maruthupandy M, Rajivgandhi GN, Quero F, Li W-J. Anti-Quorum Sensing and Anti-Biofilm Activity of Nickel Oxide Nanoparticles against Pseudomonas aeruginosa. J Environ Chem Eng. 2020;8:104533. https://doi.org/10.1016/j.jece.2020.104533
8. Abiroo J, Gulnaz B, Rubhana Q, Bashir A, Sofia AY. Modified Germ Tube Test: A Rapid Test for Differentiation of *Candida albicans* from *Candida dubliniensis*. Int J Contemp Med. 2018;5:C15-17.
9. Atiya MA, Hassan AK, Kadhim FQ. Green Synthesis of Copper Nanoparticles Using Tea Leaves Extract to Remove Ciprofloxacin (CIP) from Aqueous Media. Iraqi J Sci. 2021;2832–2854. https://doi.org/10.24996/ijs.2021.62.9.1
10. Miri A, Najafzadeh H, Darroudi M, Miri MJ, Kouhbanani MAJ, Sarani M. Iron Oxide Nanoparticles: Biosynthesis, Magnetic Behavior, Cytotoxic Effect. Chem Open. 2021;10:327–333. https://doi.org/10.1002/open.202000186
11. Sandhya J, Kalaiselvam S. Biogenic Synthesis of Magnetic Iron Oxide Nanoparticles Using Inedible Borassus Flabellifer Seed Coat: Characterization, Antimicrobial, Antioxidant Activity and in Vitro Cytotoxicity Analysis. Mater Res Express. 2020;7:015045. https://doi.org/10.1088/2053-1591/ab6642
12. Rusianto T, Wildan MW, Abraha K. Various Sizes of the Synthesized Fe_3O_4 Nanoparticles Assisted by Mechanical Vibrations. 2015
13. Ahmad S, Riaz U, Kaushik A, Alam J. Soft Template Synthesis of Super Paramagnetic Fe3O4 Nanoparticles: A Novel Technique. J Inorg Organomet Polym. 2009;19:355–360.
14. Attia NF, El-Monaem EMA, El-Aqapa HG, Elashery SEA, Eltaweil AS, El Kady M. Iron Oxide Nanoparticles and Their Pharmaceutical Applications. Appl Surf Sci Adv. 2022;11:100284. https://doi.org/10.1016/j.apsadv.2022.100284.
15. Wang L, Hu C, Shao L. The antimicrobial activity of nanoparticles: present situation and prospects for the future. Int J Nanomedicine. 2017;12:1227-1249. https://doi.org/10.2147/IJN.S121956.
16. Zúñiga-Miranda J, Guerra J, Mueller A, Mayorga-Ramos A, Carrera-Pacheco SE, Barba-Ostria C, Heredia-Moya J, Guamán LP. Iron Oxide Nanoparticles: Green Synthesis and Their Antimicrobial Activity. Nanomaterials. 2023; 13(22):2919. https://doi.org/10.3390/nano13222919.

17. Pizzino G, Irrera N, Cucinotta M, Pallio G, Mannino F, Arcoraci V, Squadrito F, Altavilla D, Bitto A. Oxidative Stress: Harms and Benefits for Human Health. Oxid Med Cell Longev. 2017;2017:8416763. https://doi.org/10.1155/2017/8416763.
18. Kong J, Fan R, Zhang Y, Jia, Z., Zhang J, Pan H, Wang Q. Oxidative stress in the brain-lung crosstalk: cellular and molecular perspectives. Front Aging Neurosci. 2024;16:1389454. https://doi.org/10.3389/fnagi.2024.1389454.
19. Abdelhamid HN, Badr G. Nanobiotechnology as a Platform for the Diagnosis of COVID-19: A Review. Nanotechnol Environ Eng. 2021;6. https://doi.org/10.1007/s41204-021-00109-0.
20. Gupta D, Boora A, Thakur A, Gupta TK. Green and sustainable synthesis of nanomaterials: Recent advancements and limitations. Environ Res. 2023;231:116316. https://doi.org/10.1016/j.envres.2023.116316.
21. Osman AI, Zhang Y, Farghali M, Rooney DW, Al-Fatesh AS, Elgarahy AM, Alharbi NS, Al-Muhtaseb AH, Jamil F, Abdulkhani A, Awad S, Abo El-Nour M, Bekheet MF, Yousef T, El-Shafay AS, Barhoum A. Synthesis of green nanoparticles for energy, biomedical, environmental, agricultural, and food applications: A review. Environ Chem Lett. 2024;22:841–887. https://doi.org/10.1007/s10311-023-01682-3.
22. Snehal S. Wagh, Vishal S. Kadam, Chaitali V. Jagtap, Dipak B. Salunkhe, Rajendra S. Patil, Habib M. Pathan, Shashikant P. Patole. Comparative Studies on Synthesis, Characterization and Photocatalytic Activity of Ag Doped ZnO Nanoparticles. ACS Omega. 2023;8(8):7779–7790. https://doi.org/10.1021/acsomega.2c07499
23. Nawaz A, Farhan A, Maqbool F, Ahmad H, Qayyum W, Ghazy E, Rahdar A, Díez-Pascual AM, Fathi-karkan S. Zinc oxide nanoparticles: Pathways to micropollutant adsorption, dye removal, and antibacterial actions - A study of mechanisms, challenges, and future prospects. J Mol Struct. 2024;1312:138545. https://doi.org/10.1016/j.molstruc.2024.138545.
24. Abisha MM, Usha D, Ashwin BM, Dennison MS. Integrating microwave-assisted green synthesis, DFT simulations, and biological activity evaluation of copper-doped zinc oxide nanoparticles. Sci Rep. 2025;15:19348. https://doi.org/10.1038/s41598-025-03922-8
25. Mishra DN, Prasad L, Suyal U. Synthesis of zinc oxide nanoparticles using Trichoderma harzianum and its bio-efficacy on Alternaria brassicae. Front Microbiol. 2025;16:1506695. https://doi.org/10.3389/fmicb.2025.1506695.